Non-linear Soil-Structure Interaction of Bridge Foundations in highly Seismic Regions

Phil Clayton[1], Ronald Wessel[2], Anton Kivell[3], Jamil Khan[4]

ABSTRACT: *A new expressway section with 17 bridges passing through the Kāpiti Coast Region is under construction and forms part of State Highway 1- Wellington Northern Corridor which is part of NZTA's Roads of National Significance program. The high seismicity of the Kāpiti Coast produces design peak ground accelerations of up to 0.98g in a 1/2500 year design event. Very high seismicity combined with liquefiable ground conditions required a detailed understanding of non-linear soil structure interaction to develop bridge design concepts, in particular for the abutments and piers. This paper presents design concepts and practical modelling techniques which have been applied in the design to accommodate non-linear soil behaviour and a ductile structural response, using one of the major bridge structures as an example.*

KEYWORDS: Non-linear soil-structure interaction, ductile behaviour of piles , seismic design of bridges for liquefaction , performance based seismic design

[1] Phil Clayton , Associate Geotechnical Engineering, BECA Ltd., Email: phil.clayton@beca.com
[2] Ronald Wessel, Senior Bridge Engineer, BECA Ltd. Email : ronald.wessel@beca.com
[3] Anton Kivell, Structural Engineer, BECA Ltd. Email: anton.kivell@beca.com
[4] Jamil Khan, Associate - Structural Engineering, BECA Ltd., Email: jamil.khan@beca.com

1 INTRODUCTION

A new expressway is currently under construction within the Kāpiti Coast Region of Wellington, New Zealand. The Mackays to Peka Peka (M2PP) expressway project involves 15 road and a number of pedestrian and cycleway bridges and is the first section to be constructed within the State Highway 1- Wellington Northern Corridor, one of the seven Roads of National Significance (RoNs) under the New Zealand Transport Agency's (NZTA) RoNS Program. The program comprises seven projects based around New Zealand's five largest population centres. The focus is on moving people and freight between and within these centres more safely and efficiently. After a major earthquake, the expressway is to provide a life-line route throughout the Wellington Northern Corridor, along the Kāpiti Coast, providing access to the City of Wellington, New Zealand's capital.

The high seismicity of the Kāpiti Coast region results in design peak ground accelerations of up to 0.98g in a 1/2500 year ultimate limit state (ULS) design event and 0.29g in a 1/100 year serviceability limit state (SLS) event. Extensive sections of the route are underlain by potentially liquefiable dune sands and silts interspersed by peat deposits. Very high seismicity combined with liquefiable ground conditions required a detailed understanding of non-linear soil structure interaction to evaluate options for and to design the bridges, in particular their substructures. Waikanae River Crossing, which is one of the first structures to be constructed, is used as a case study in the following to illustrate design concepts and modelling techniques which have been applied in the design.

2 Waikanae River Crossing

Waikanae River Bridge comprises of twin bridges carrying separately the northbound and southbound carriageway of the Expressway over Waikanae River and its associated flood plain. It also carries a combined pedestrian cycle way.

The bridge comprises of 5 simply supported spans ranging from 32m to 38m span length with a total length of 181m between abutment faces. Figure 1 and Figure 2 show a pier and abutment cross section respectively.

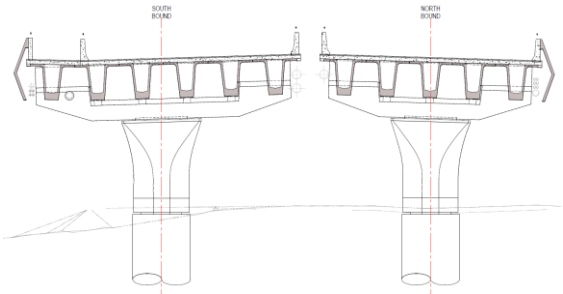

Figure 1: *Typical Pier Cross section of Waikanae River Crossing*

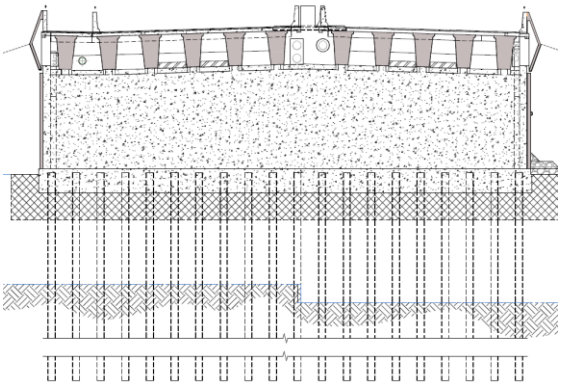

Figure 2: *South Abutment Cross Section of Waikanae River Crossing*

3 Analytical Approaches Adopted to Consider Soil-Structure Interaction

3.1 Analytical Representation of Soil Response

In the past modelling of non-linear soil responses has been undertaken by approximating the non-linear behaviour of soil with linear Winkler springs [1]. Multi-linear soil springs are more rarely used due to the limitations of most structural engineering analysis packages. On the M2PP project, during the concept of confirmation design stage, the design team modelled non-linear behaviour through iterative elastic analysis until displacement compatibility was achieved [2].

During the detailed design stage soil response was modelled using p-y-curves [1,2] derived in the geotechnical software package L-Pile [3]. The soil profile at each pile location was simplified into horizontal layers with similar strength/density and the most appropriate p-y response model selected. Response models were selected as follows:

- Sands and silty sands utilised a model published in [4]
- Plastic silts and clays utilised a model published in [5]
- Liquefied sand utilised a model published in [6]

A range of soil properties comprising bulk density (overburden stress), friction angle or undrained shear strength were then utilised to factor the soil model and generate the P-Y curves. For each layer 'nominal', 'hard' and 'soft' values were derived to reflect the likely range of soil properties. This approach was taken to consider a 'most likely' behaviour alongside a case likely to result in upper bound deflections i.e. the 'soft' case and upper bound actions i.e. the 'hard' case.
The P-Y curves were then utilised in two different ways, either within subsidiary analyses to derive a pile top response matrix or as inputs to a global analysis.

3.2 Direct 2D-Representation of P-Y Curves

This approach, suggested in [7] involves substituting a pile (reinforced concrete or steel) embedded in a given soil profile with a non-linear translational and rotational spring matrix for analysis. Refer to Figure 3.

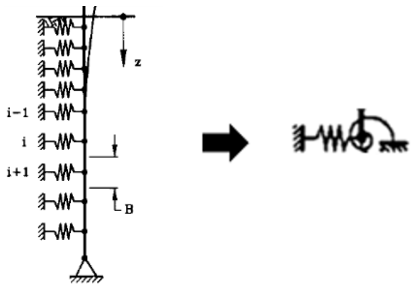

Figure 3: *Substitution of Pile Soil Springs with single pile head spring [7]*

3.2.1 Modelling of Piers

At the pier locations, where reinforced concrete mono piles were employed, the spring characteristics were derived in L-Pile by modelling the stiffness characteristics of the pile (refer to Figure 4) and applying shear and flexure increments to the pile head.

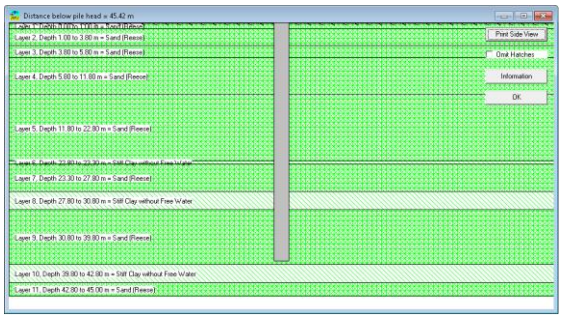

Figure 4: *Screenshot of a Reinforced Concrete Pile Modelled in a given soil Profile [3]*

The flexure and shear effects were proportioned to match that as expected by the structural system, e.g. as shown in Figure 5 a cantilever moment being proportional to the distance from the pile head to the centroid of the seismic mass and application of the base shear.

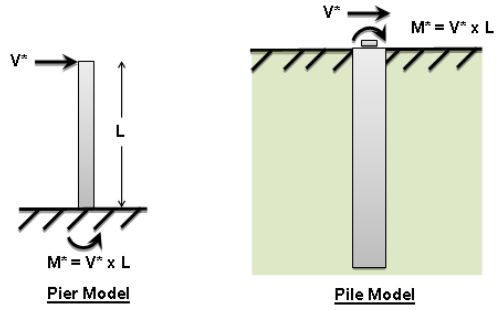

Figure 5: *Application of Shear and Flexure to pile in L-PILE [3]*

At each increment shear-displacement and moment-rotation relationships were recorded, until yielding of the pile occurred. The resulting shear-displacement and moment-rotation plots defined the characteristics of the pile head spring.

3.2.2 Modelling of Abutments

At the abutments the principal concept consists of a pile group with 2 rows of steel H-piles tied into a reinforced concrete pile cap. Due to the relatively insignificant stiffness of the steel piles to the pile cap, pile head fixity was assumed.
In L-PILE, the pile group was reduced to a single pile whilst accounting for pile shadowing effects of adjacent piles.
With the pile head assumed fixed against rotation and all piles assumed to translate uniformly as a pile group, only displacement increments needed to be applied to the pile head to compile shear-displacement and moment– rotation characteristics.

3.3 Simplification of P-Y curves to Tri-Linear Springs

In the concept confirmation stage of the design p-y curves were simplified for ease of analysis to non-linear springs. In this regard tri linear curves were selected to maintain the core characteristics of the curve without excessive iteration [2]. The three principal segments of the p-y curve (granular soil) consist of the initial elastic stiffness, the large strain stiffness and the ultimate soil resistance as shown in Figure 6.

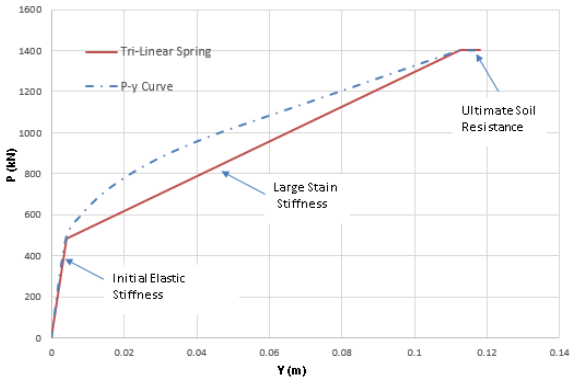

Figure 6: *Three principal segments of a P-Y-curve for Granular Soil type not subject to liquefaction*

A similar three segment approach was taken to represent the concave upward p-y curves of liquefiable sands as shown in Figure 7.

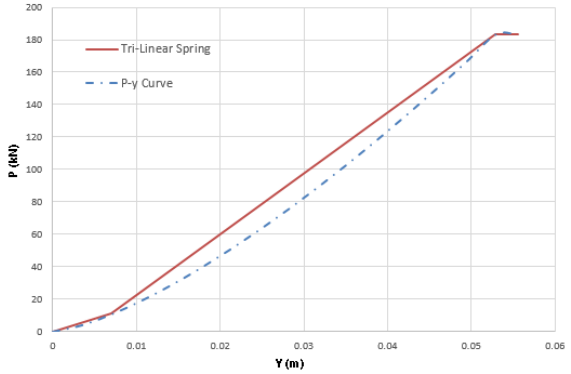

Figure 7: *Concave upward p-y curves of liquefiable sands.*

3.4 Consideration of the Hard and Soft Soil Stiffness

For both approaches hard (most likely upper bound) and soft (most likely lower bound) soil response properties were considered to account for a possible range of soil responses and the potential for soil stiffness to degrade during shaking, as liquefaction may not initiate on the first shaking cycle.

3.4.1 The Initiation of Liquefaction

Liquefaction assessment for the site has been undertaken generally in accordance with the recommendations in [8], modified by the recommendations in [9].

3.4.2 Pile Shadowing

"Pile shadowing", the reduction in lateral stiffness and capacity due to interaction of piles within a laterally loaded pile group, was accounted for by reducing the effective modulus of horizontal subgrade reaction and the ultimate capacity of springs, the so called 'P-multiplier' approach [10]. When adopting a p-y curve analysis, the force component of a particular p-y curve was scaled down in L-PILE through the use of a 'P multiplier'. Utilising a simplification of the approach in [10], the scale factor was determined on the assumption that full capacity and stiffness is achieved when the spacing of the piles is 8D or more in a longitudinal direction and 3D or more in a transverse direction, where D is the cross section of the pile. Reduction factors were applied, which varied depending on the load case (the soil loading the piles or the piles loading the soil) and for lagging or leading piles in the group.

4 Embankment Behaviour at Abutments

Given the high seismicity even at minor seismic events and the added risk of liquefaction, it was necessary to assess the embankment displacement behaviour in order to assess the level of damage to the approach embankments in a minor and major event as well any impact on the bridge abutments.
Displacement assessments were based on Newmark sliding block theory [11,12] utilising coseismic displacement regression analyses published in [13] in conjunction with yield accelerations computed in the geotechnical software package Geostudio Slope/W [14].
Preliminary analyses estimated embankment displacements of greater than 1m for some bridge abutments due to liquefaction effects. Consequently ground improvement was found to be necessary beneath most abutments to reduce embankment displacements to more viable design levels of 50-150mm. In the course of this process a range of displacement mechanisms had been considered,
Figure *8* and Figure 9 show shallow and deep slip planes under liquefied conditions at the Waikanae River Crossing.

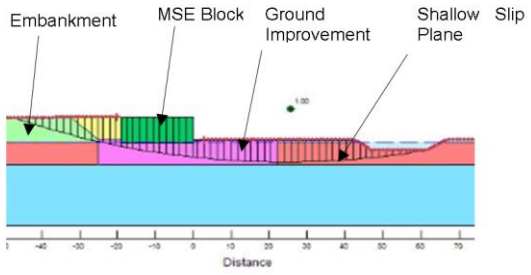

Figure 8: *Illustration of stability analysis carried out for Waikanae River Bridge under a shallow seated mechanism [14].*

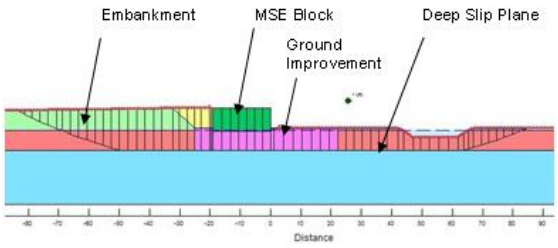

Figure 9: *Illustration of stability analysis carried out for Waikanae River Bridge under a deeper seated mechanism along top of dense gravel layer [14].*

5 Design Concepts for Abutments

In the light of the still significant embankment displacements of 50-150mm, two principal design concepts were considered. The first concept comprised a series of reinforced concrete piles in steel sleeves to accommodate embankment movement. The second concept allowed the abutment to move with the embankment while utilising compact section steel piles to maintain vertical support.

The second solution was considered more cost effective due to substantial savings in materials and installation time and was therefore selected for further refinement with a focus on the displacement performance of the steel H-piles.

Steel Piles were considered inherently more ductile due to their significant inelastic rotation capacity as suggested in [15], provided a compact section is used. Furthermore, buried steel H piles are not subjected to the durability concerns of reinforced concrete piles in the event of significant plastic hinging taking place.

The displacement performance was found to depend on several factors which are discussed further below.

5.1 Relationship between Vertical Load Demand and Inelastic Rotation Capacity

A correlation between the level of axial load force applied and the inelastic rotation capacity is provided in [15].

In this regard it is distinguished between earthquake related (cyclic) movements and monotonic movements caused by other actions. This distinction is relevant since the inelastic rotation capacity of a compact steel section under monotonic movement is considered 30% greater than under cyclic movement.

For a steel member with an axial demand of 15% or less of the structural axial capacity, the allowable rotation in a plastic hinge is 0.06 radians at ultimate limit state, which in this case, is caused by (monotonic) embankment displacements in the course of a seismic 1/2500yr design event.

The abutment piles have therefore been sized to utilise the maximum allowable rotation capacity by limiting the average utilisation to15% of the section axial capacity under gravity loading.

5.2 Range of Sliding Block Mechanisms

Based on slope analysis, carried out in Geostudio SLOPE/W [14], embankment displacements of between 50mm and 150mm are typically estimated for longitudinal slip planes occurring between the underside of the MSE Block and the top of the dense granular soils at depth (refer to Figure 10 and Figure 11). With the largest displacements anticipated toward the base of this zone, other seismic actions are expected to be less where estimated displacements are greatest. On this basis the peak displacement demand and associated flexure and shear demand imposed on a steel pile due to sliding block mechanisms at depth could be either considered in isolation to any other seismic demands transferred to the 'H' piles near ground level or at the very least had a less compounding effect when combined with any other seismic action.

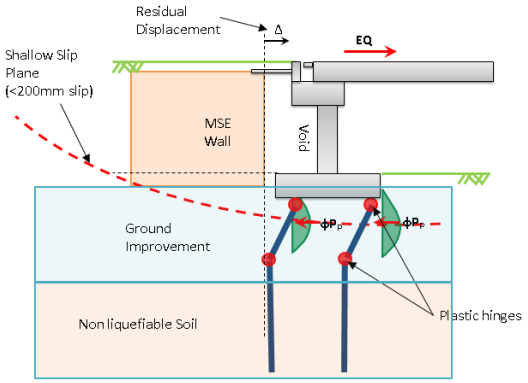

Figure 10: *Assessment of Steel Pile Performance subject to Range of Sliding Block Mechanisms (here inertia effects and embankment sliding are shown in phase).*

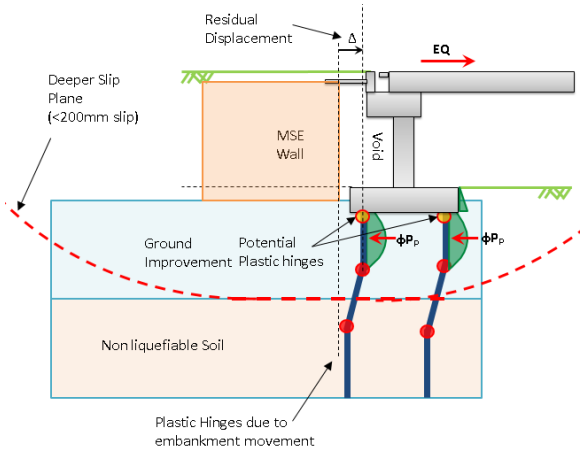

Figure 11: *Assessment of Steel Pile Performance subject to Range of Sliding Block Mechanisms*

(here inertia effects and embankment sliding are shown in phase).

5.3 Steel Pile Orientation

For Waikanae River Crossing 410mm deep steel H pile sections were employed due to better drivability characteristics than similar sized closed sections in gravel layers.

Due to the geometry of the H piles, the stiffness and yield moment capacity are greater about the major axis than about the minor axis. Therefore, where very well confined in dense soil the potential of shear failure of the pile about the major axis before ductile failure, i.e. before exceedance of the yield moment capacity and plastic hinge formation is greater, subject to the distance of peak flexure demands along the depth of the piles.

In light of this, the steel 'H' piles are orientated with the minor rotation axis towards the longitudinal direction as in this direction displacement demands due to both abutment displacement and inertial effects are greater.

5.4 Overburden Pressure

As part of the analyses a specific check has been undertaken to confirm that the buckling moment capacity of the compact section 'H' piles exceeded the yield moment capacity to ensure a ductile hinge mechanism. This check was undertaken by imposing a 'shear' offset in the soil of 200mm while assuming that the surrounding soil provided restraint/loads to the H piles utilising P-Y curves derived in LPILE [3].

These analyses revealed that with increased overburden pressure, and resulting stiffer soils, the distance between plastic hinges reduced. The inelastic displacement capacity of the 'H' piles under nominal soil conditions varied between 84mm and 130mm depending on the overburden pressure assumed. The variation in displacement capacities of an H pile performing under a range of overburden pressures are illustrated in Figure 12.

In this figure 100% overburden pressure is equal to the full embankment height. Subject to the position and distance of a particular H-pile to the MSE block, the magnitude of overburden pressure varies. Based on a simplification of the pressure distribution is was assumed that most of the front row of steel piles experiences only 50% of full overburden pressure, the corner piles only 25% and most of the back row about 75% of the full overburden pressure induced by the MSE block. A pragmatic approach was taken by using the mean total displacement capacity (elastic displacements plus inelastic displacement capacity) of 150mm for further assessment purposes.

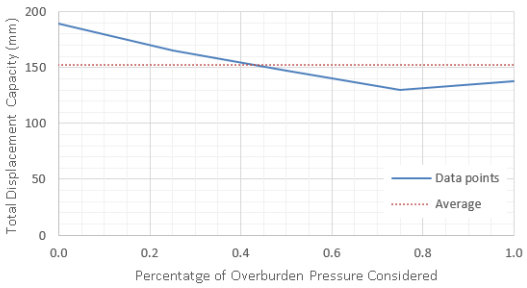

Figure 12:*Effect of Overburden Pressure on Displacement Capacity*

6 Design Concepts for Piers

6.1 Seismic Related Actions Considered

Seismic related actions on the piers originate from a number of possible sources including structural inertia effects resulting from the seismic mass of the structure, lateral spreading and the kinematic effects of cyclic ground movements (ground lurching). In the absence of ground improvement liquefaction occurs at most of the pier locations.

6.1.1 Inertia Effects

Inertia effects were assessed using a displacement based design approach which is extensively discussed in [16] and drafted as an Appendix [17] to compliment the current edition of NZTA Bridge Manual [18]. The displacement based design procedure requires normalised response spectra as provided in [20], or specific for the project in [19] to be converted to equivalent normalised displacement demand spectra. Figure 13 compares normalised displacement spectra of major Australian and New Zealand cities for subsoil class D/De and a 1/2500yr event with a probability factor R= 1.65 based on [19] and R= 1.8 used for the other locations [20,21].

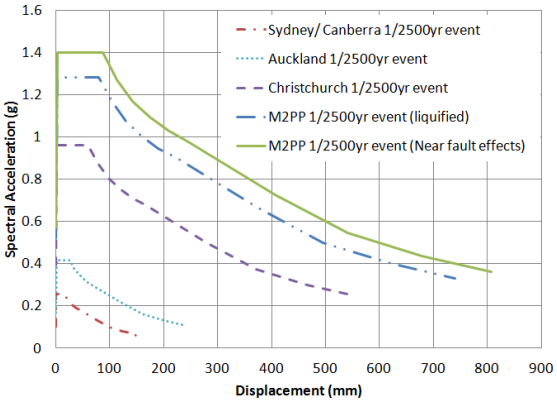

Figure 13: *Normalised Displacement Demand Spectra in Comparison based on [19,20,21]*

Waikanae River Crossing has simply supported spans with similar column heights at all piers. In this instance, the superstructure could be reduced to

a lump mass in a single degree of freedom system for further analysis in the longitudinal direction.
In the transverse direction, a non-linear pushover analysis was undertaken by modelling the pier substructure above ground level and substituting the pile foundations with non-linear springs.

6.1.2 Hinging of Reinforced Concrete Piles

[18] and [22] allows economy in the design of pile reinforcement by allowing the formation of plastic hinges at depth i.e. deriving an inelastic displacement capacity which contributes to satisfying the spectral displacement demands in lieu of an increase in flexural section capacity.
In this regard [18,22] limit the level of plastic hinging by limiting the level of displacement ductility to less than 3 which defines the upper boundary of limited ductility in [23]. The limit on displacement ductility implies that pile hinging is acceptable within the strain limits and resulting curvature limits as defined in [23] when assuming limited ductility.
The strain limits associated with the curvature limits appear significantly higher than strain limits of ε_c=0.008 and ε_s=0.015 with ε_c being the limiting concrete strain and ε_s being the limiting steel strain suggested in [16, 24] for piles hinging at depth. What compensates for the suggested lower strain limits is the difference in the approach of deriving the plastic hinge length required to calculate the inelastic rotation and displacement capacity: Based on [23] the plastic hinge length L_p for a pile is $h_c/2$, whereby h_c is in this case the pile diameter. Based on [16] however L_p can be calculated as (for definition of terms refer to Figure 14):

$$L_p = D + 0.1\left(H - H_{cp}\right) \leq 1.6D \qquad (1)$$

with H_{cp} = 0 for cantilever columns.

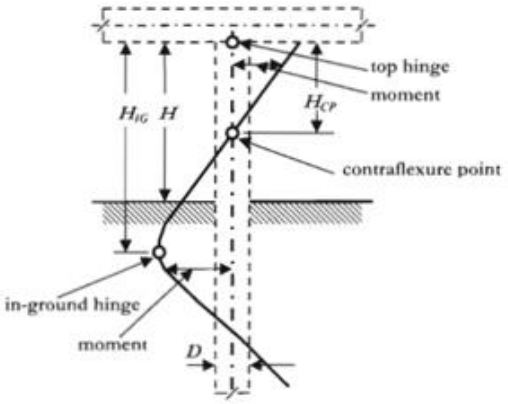

Figure 14: *Plastic hinge length for hinge at depth [16]*

Hence L_p is up to three times greater than the value derived from the code.

6.1.3 Lateral Spreading

Analysis of lateral spreading potential at piers has been undertaken on selected bridges where flow of unimproved ground has the potential to apply lateral loads to bridge piers. For the Waikanae River Crossing an upperbound check was carried out considering the potential for lateral spreading resulting from a 7m deep potentially liquefiable layer and a 'free face' in the river channel. Analyses conservatively assumed non-liquefied soil properties, applying 1m of soil displacement over the upper 7.0m of the pile. Refer to Figure 15. The resulting flexural demands load effects comprised only 25% of the flexural pile capacity and resulted in a deflection at the pile head of around 50mm.

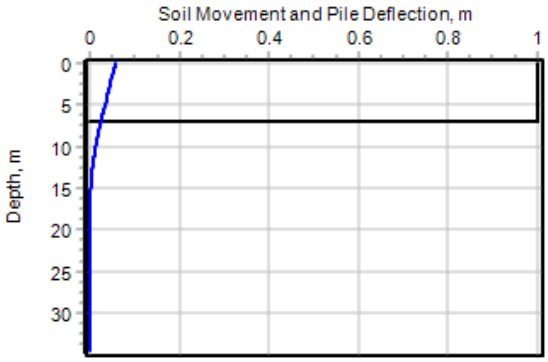

Figure 15: *Lateral Spreading Analysis in L-PILE [3]*

6.1.4 Ground Lurching

Under liquefied conditions, cyclic soil displacements can be significant, resulting in high kinematic loads. As the soil column oscillates it imposes significant soil pressure (up to passive pressure depending on the pile stiffness) on the pile [25].
A cumulative cyclic strain profile derived using the methodology in [25] was applied in L-Pile to the pier piles under liquefied conditions.

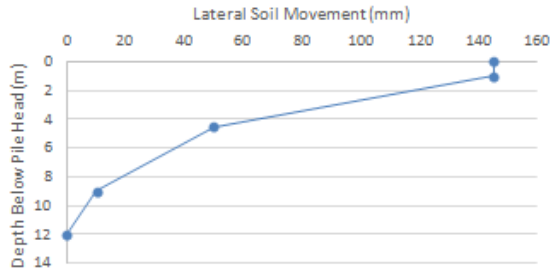

Figure 16: *Cyclic Strain Induced Soil Displacements applied to pier pile*

The resulting load effects can be significant (M= 10.000kNm for a 3m diameter pile) however due to the large diameter of the pier piles relative to the depth of liquefaction these demands were found to be small compared to the capacity of the pile. However for smaller piles, or greater depths of liquefaction these effects could be significant.

Note that peak inertia effects, lateral spreading and ground lurching were not considered to act concurrently [26].

6.2 Interaction of Pier and Abutment Behaviour in a Seismic Event

6.2.1 Interaction in the Longitudinal Direction

Most bridge structures are multi-span bridges ranging between 2 to 5 spans. In these cases the bridge decks are effectively decoupled from the abutments by introducing low friction free sliding bearings at the abutments. The decoupled articulation allows an out-of-phase displacement behaviour of the bridge deck relative to the abutment and therefore does not create additional longitudinal displacement demands for the steel H-piles.

6.2.2 Interaction in the Transverse Direction

[16] and the commentary to [17] describe various deck displacement behaviours subject to the level of restraint of the deck to the abutment as illustrated in Figure 17 for a hammerhead type pier substructure with a single column per pier.

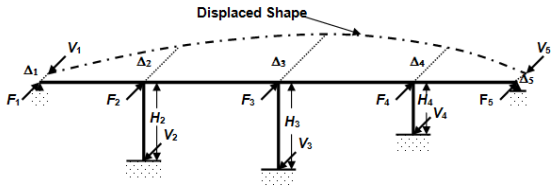

Figure 17: *Deck Displacement Behaviour subject to abutment restraint [16, 17]*

For Waikanae River Crossing a design philosophy with controlled failure of transverse restraints has been adopted: steel shear key brackets at the abutments provide restraint under a minor (SLS) seismic event, but are sheared off once a defined seismic response of the bridge deck, i.e. a specific seismic induced acceleration, is exceeded. In this event, the bridge deck is then only restrained by the friction at deck beam soffit and abutment shelf interface. The end-spans of the bridge deck thus act as lateral cantilevers to the pier which is closest to the abutment. This design concept achieves two goals: the level of transverse base shear transferred to abutments and steel piles is capped, and the level of out of plane flexure resisted by the end-spans at the adjacent piers does not depend on the seismic response but only on the friction demand. The resulting deck displacement behaviour is illustrated in Figure 18.

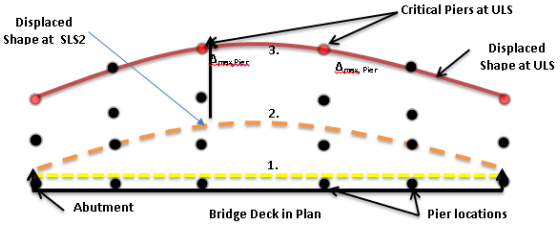

Figure 18: *Anticipated Displacement Behaviour at Waikanae River Bridge: 1.) Bearing Displacements 2.) Deck Displacements at SLS 3.) Abutment Shear keys are sheared off at ULS and deck displaces transversely.*

6.2.3 Combination of Inertia and Ground Movement - Transverse

For vertical abutments with a pile cap footing supported by steel H-piles as shown in Figure 11, the abutment wall and the approach ramp are partially decoupled. For this case a soil friction design concept was adopted which assumes that the MSE block and underlying soil will, at most, exert friction loads onto the back of the H-piles underneath the base of the abutment. The friction surface is illustrated in Figure 19.

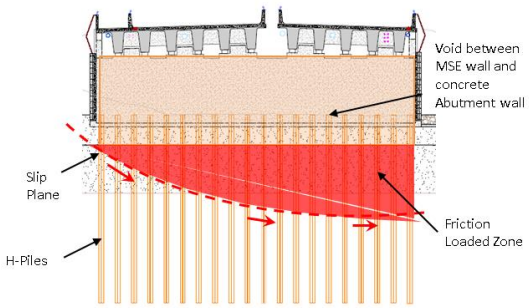

Figure 19: *H piles exposed to friction loads due to Sliding Embankment*

The friction loads resulting from a transverse embankment movement have been determined based on the shear strength of soil beneath the MSE block.

When combining the transverse friction loading with inertial loading three possible scenarios were considered:

- Where inertial pile movement in the direction of soil movement increased the soil movement (in-phase, the piles displace less than the soil).
- Where pile movement and soil movement are the same then the frictional force is zero (pile movement matches the soil movement).
- Where the soil friction will assist in resisting the inertial load, if the pile moves further than the soil movement due to inertial loading.

Based on the steel H pile analysis carried out with L-Pile, the transverse pile movement was significantly less (up to 30mm) than the transverse embankment movement of 150mm. Therefore, friction loads were combined with inertia loads.

7 CONCLUSIONS

Very high seismicity combined with liquefiable ground conditions encountered in the design of the new M2PP Expressway project required the designers to develop a detailed understanding of

non-linear soil structure interaction to develop bridge design concepts, in particular for the substructure. This paper has presented design concepts and practical modelling techniques adopted for the project to accommodate non-linear soil behaviour and ductile structural response in the design of bridges for the combined high seismicity and liquefaction.

Aspects considered include the development of articulation concepts for the bridge substructures with consideration of ground lurching, lateral spreading, embankment sliding, longitudinal in-phase and out-of-phase interaction of the bridge deck to the abutments as well as the need to cater for the load transfer of the longitudinal and transverse response of the bridge deck to the abutments.

ACKNOWLEDGEMENT

The authors would like to acknowledge the client NZTA, the construction team lead by Fletcher Construction Ltd. and colleagues of the structural and geotechnical design team which have contributed to the key findings summarised in this paper.

REFERENCES

[1] Elson W.K.: Report 103 – Design of Laterally Loaded Piles, Construction Industry Research and Information Association(Ciria), London, 1984

[2] Kramer S.L: Development of P-y Curves for Analysis of Laterally Loaded Piles in Western Washington, Washington State Department of Transportation, Washington, 1988

[3] Ensoft, Inc,: LPILE, 2013 .

[4] Reese, L. C., Cox, W. R., and Koop, F. D.: Analysis of laterally loaded piles in sand, Proc. 6th Offshore Technology Conference, Paper 2080, Houston, Texas, 473-483. , 1974

[5] Matlock, H.: Correlations for Design of Laterally Loaded Piles in Soft Clay, 2nd Annual Offshore Technology Conference, Houston, Texas, pp 577 - 594 , 1970

[6] Rollins, K.M., Gerber, T.M., Lane, J.D., and Ashford, S.A.: Lateral Resistance of a Full-Scale Pile Group in Liquefied Sand, J. of Geotech. and Geoenviron. Engineering, ASCE, 131(1) , 2005

[7] Priestley M. J. N., Calvi G.M., Seible F.: Seismic Design and Retrofit of Bridges, Wiley & Sons, New York, Chichester, Brisbane, Toronto, Singapore, 1996

[8] Idriss, I.M. & Boulanger, R.W.: Soil Liquefaction during Earthquakes: MNO-12. Earthquake Engineering Research Institute, Oakland, CA. , 2008

[9] Robertson, P.K. and Cabal, K.L.: Guide to Cone Penetration Testing for Geotechnical Engineering, Prepared for Gregg Drilling & Testing Inc., 5 th Edition, , p. 130, 2012

[10] Mokwa, R.L: Investigation of the resistance of pile caps to lateral loading. Faculty of the Virginia Polytechnic Institute and State University, Blacksburg, Virginia, PP 6-74., 1999

[11] Newmark N.M: Effects on Dams and Embankments, 5th Rankine Lecture, Institution of Civil Engineers, London, 1965

[12] Kramer S.L.: Geotechnical Earthquake Engineering, Prentice-Hall, University of Washington, 1996

[13] Jibson R.W.: Regression models for estimating coseismic landslide displacement. Engineering Geology, Vol 91, Issues 2-4, pp. 209-218. , 2007

[14] Geoslope, Geostudio Slope/W. , 2012

[15] Standards New Zealand, NZS 3404:1997 Steel Structures Standard, 1997

[16] Priestley M. J. N., Calvi G.M., Kowalsky M. J.: Displacement Based Design of Structures, IUSS Press, Pavia, 2007

[17] New Zealand Transport Agency (NZTA) Bridge Manual Draft Appendix A: Proposed Provision for Deflection Based Design, Draft DBD7, 23rd February 2013

[18] New Zealand Transport Agency (NZTA) : Bridge Manual third Edition, May 2012

[19] Jury R, Bothara J.: Site Specific Seismic Hazard Assessment Study for Meckays to Peke Peka Expressway, BECA Ltd , Wellington, 2012

[20] Standards New Zealand, NZS 1170.5:2004 – Structural Design Actions, Part 5: Earthquake actions – New Zealand, 2004

[21] Standards New Zealand, AS 1170.4:2004 – Structural Design Actions, Part 4: Earthquake actions – Australia, 2004

[22] Transit New Zealand: Bridge Manual second Edition, 2003

[23] Standards New Zealand, NZS 3101:2006, Concrete Structures Standard, Part 1 – Design of Concrete Structures, 2006

[24] Priestley M. N : Advice to NZTA via Email Correspondence, 20th February 2014

[25] Tokimatsu, K. and Asaka, Y.: Effects of Liquefaction-induced ground displacements on Pile Performance in the 1995 Hyogoken Nambu Earthquake, Soils and Foundations, Special Issue, pp. 163–177, 1998

[26] ATC/MCEER: Recommended LRFD Guidelines for the Seismic Design of Highway Bridges. By Applied Technology Council/Multidisciplinary Center for Earthquake Engineering Research Joint Venture for the National Cooperative Highway Research Program, Washington, DC. , 2003